Glacial Effects on Discharge and Sediment Load in the Subarctic Tanana River Basin, Alaska

Authors: Wada, Tomoyuki, Chikita, K. A., Kim, Y., and Kudo, I.

Source: Arctic, Antarctic, and Alpine Research, 43(4) : 632-648

Published By: Institute of Arctic and Alpine Research (INSTAAR), University of Colorado

URL: https://doi.org/10.1657/1938-4246-43.4.632

Arctic, Antarctic, and Alpine Research, Vol. 43, No. 4, 2011, pp. 632–648

Glacial Effects on Discharge and Sediment Load in the Subarctic Tanana River Basin, Alaska

*Tomoyuki Wada**
*K. A. Chikita**§
Y. Kim† and
I. Kudo‡

*Faculty of Science, Hokkaido University, Sapporo, 060-0810, Japan
†The International Arctic Research Center, the University of Alaska Fairbanks, Fairbanks, Alaska, 99775-7340, U.S.A.
‡Faculty of Fisheries Sciences, Hokkaido University, Hakodate, 041-8611, Japan
§Corresponding author: chikita@mail.sci.hokudai.ac.jp

Abstract

About 5.6% of the drainage area of the Tanana River, Alaska, is covered by mountainous glacierized regions, and most of the other area by forests (51%) and wetlands (9%) with discontinuous permafrost. The water discharge and sediment load from glacierized and non-glacierized regions within the drainage area were represented by observed data of the proglacial Phelan Creek and the non-glacial Chena River, respectively, which are both the tributaries of the Tanana River and ultimately drain to the Yukon river basin. In the glacier-melt periods of 2007 and 2008, the runoff rate and suspended sediment concentration in Phelan Creek was 15 times and 36 times as high as those in the non-glacial Chena River, respectively. As a result, the mean sediment yield in the glacier-melt periods of 2007 and 2008 for Phelan Creek (24.8 t km^{-2} day^{-1}) was estimated to be 640 times as high as that in the Chena River (0.039 t km^{-2} day^{-1}). Hence, the glacierized regions were considered to be a major source of the fluvial sediment. In order to quantify the contribution of water discharge and sediment load from the glacierized regions to those of the Tanana River, the time series of water discharge, Q, and sediment load, L, in the glacier-melt periods were simulated by a tank model coupled with the L-Q equations (Nash-Sutcliffe efficiency coefficients, 0.41 to 0.82). The model indicates that the glacier-melt discharge accounted for 26–57% of the Tanana discharge, while the sediment load from the glacierized regions solely accounted for 76–94% of the Tanana sediment load. The remaining contribution (6–24%) of the sediment load was probably due to the fluvial resuspension of glacial sediment deposited previously in the river channels.

DOI: 10.1657/1938-4246-43.4.632

Introduction

About 11% of the global river discharge is accounted for by the discharge from the arctic river basins of the Ob, Yenisei, Lena, and Mackenzie Rivers, with spacious permafrost regions (Lammers et al., 2001). The subarctic Yukon river basin in Alaska is characterized by vast discontinuous permafrost regions and mountainous glacierized regions. The glacierized regions occupy only 1.1% of the drainage area, but can potentially yield a large amount of fine sediment through glacial erosion (Brabets et al., 2000; Chikita et al., 2002, 2007; Hasholt et al., 2006). The fine sediment input to the ocean could affect the marine primary production, since the sediment contains the nutrients of nitrogen, phosphorus, and silicate. From the viewpoint of the marine ecosystem, it is thus very important to understand the mechanisms of sediment transports in subarctic to arctic river basins.

Moreover, global warming continues, and the discharge and sediment load from glacierized regions in the world could change greatly (Global Carbon Project, 2006). Stafford et al. (2000) reported that the mean air temperature increment for the latter half of the 20th century was 1.9 °C in interior Alaska. Meanwhile, total annual discharge to the Arctic Ocean increased at 5.6 km^3 $year^{-2}$ during 1964–2000 (McClelland et al., 2006), and annual discharge from the Yukon river basin increased by 7% for 1977–2007 (Overeem and Syvitski, 2010). This discharge increment could cause the sediment load increment.

Annual sediment load from the high-latitude regions to the ocean is 347 Mt $year^{-1}$ for the Arctic Ocean, 88 Mt $year^{-1}$ for the Pacific Ocean, and 53 Mt $year^{-1}$ for the Atlantic Ocean (Overeem and Syvitski, 2008). Especially, specific sediment yield (t km^{-2} $year^{-1}$) in Alaska is by an order of $10–10^3$ higher than in Siberia (Walling and Webb, 1996). Meybeck and Ragu (1996) and Striegel et al. (2007) pointed out that, in spite of a comparable runoff rate (Yukon, 236 mm $year^{-1}$; Lena, 211 mm $year^{-1}$; Yenisei, 239 mm $year^{-1}$; Ob, 135 mm $year^{-1}$), the sediment yield in the Yukon river basin (72.2 t km^{-2} $year^{-1}$), including the Tanana River, is much higher than in the Siberian river basins (Lena, 8.3 t km^{-2} $year^{-1}$; Yenisei, 1.8 t km^{-2} $year^{-1}$; Ob, 5.2 t km^{-2} $year^{-1}$). The Mackenzie River basin also exhibits a sediment yield (66.5 t km^{-2} $year^{-1}$; Carson et al. 1998) much higher than in the Siberian river basins, in spite of a comparable runoff rate (172 mm $year^{-1}$). It is hypothesized that these high sediment yields are due to relatively high sediment yield in the glacierized regions (Yukon river basin) or the erosion of glacial tills yielded in the past (Mackenzie River basin). The high sediment yield in glacierized regions is exemplified in Greenland. Annual sediment yield (7700 to 49,100 t km^{-2} $year^{-1}$) at the Kuannersuit Glacier, Greenland, is of the order of $10^3–10^4$ higher than in the Siberian river basins (Knudsen et al., 2007). In Ammassalik Island, SE Greenland, ca. 90% of sediment load to the sea was derived from glacial erosion, in spite of 17% glacierized area in the island (Hasholt and Mernild, 2008).

1523-0430/11 $7.00

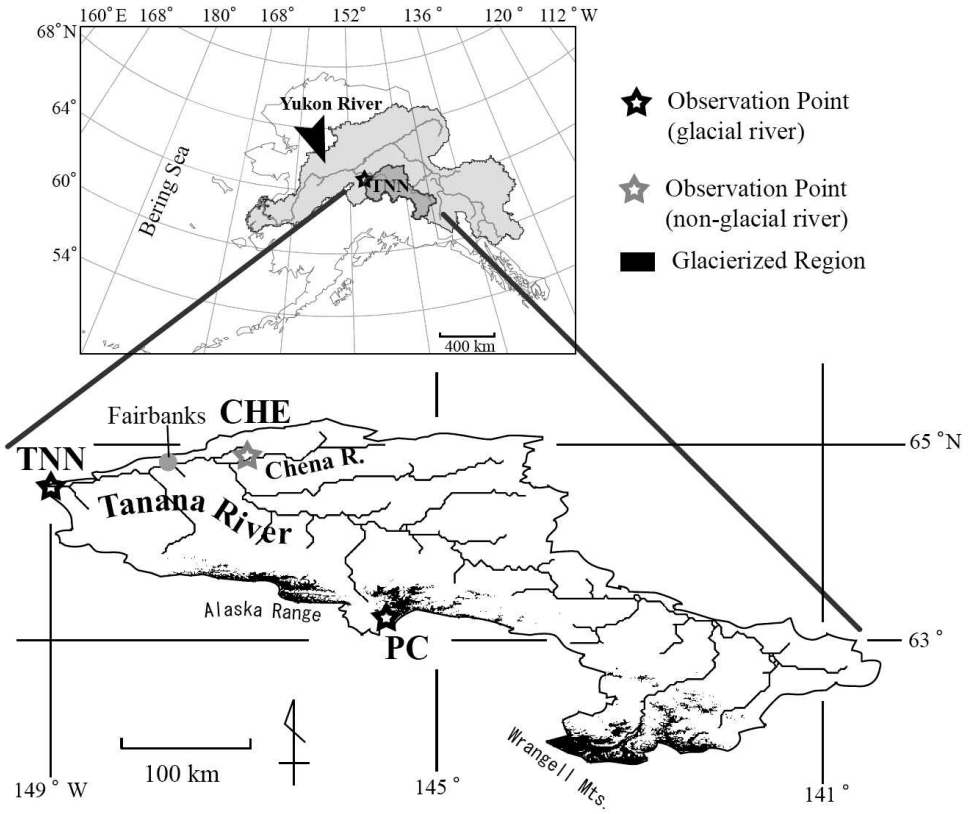

FIGURE 1. Location of the drainage basin of the Tanana River in the Yukon river basin, Alaska (upper), and observation points, TNN, CHE, and PC in the Tanana River basin (lower).

There are many studies about the fluxes of the Yukon and its tributaries (Guo and Macdonald, 2006; Striegel et al., 2007; Hay and McCabe, 2010) and a few studies about the contribution of glacier-melt discharge to river discharge (Hagg et al., 2006; Nolin et al., 2010), but few studies about the glacial impact to both discharge and sediment load (Chikita et al., 2007). In order to better predict the effect of regime changes, understanding the influence of the glacierized regions on discharge and sediment load is important. Hence, the objectives of this study are to identify the sediment source in the Tanana River basin, and to quantify the relative contributions of glacierized regions to discharge and sediment load. The Tanana River basin accounts for ca. 40% of the glacierized area of the Yukon river basin.

Study Area

Figure 1 shows the location of the Tanana River basin in the Yukon river basin, Alaska, and our three observation points in the Tanana basin. The observation points are located on the Tanana River (point TNN), in the non-glacial Chena River (point CHE), and in the proglacial Phelan Creek (point PC) in the glacierized headwater region. The Chena River basin (area: ca. 5.40×10^3 km^2, altitude: 130–1600 m a.s.l., upstream of point CHE) is a typical non-glacial river basin covered dominantly by forest with discontinuous permafrost (Ferrians, 1965). Phelan Creek is generated by discharge from the Gulkana Glacier (Kido et al., 2007; Chikita et al., 2010). The drainage area upstream of point TNN is 6.63×10^4 km^2, ranging from 100 m a.s.l. (point TNN) to 4900 m a.s.l. in altitude. The glacierized regions are situated in the Alaska Range and Wrangell Mountains above 800 m a.s.l. The mean annual precipitation for 1951–1980 in the river basin ranges from ca. 260 mm year^{-1} near point TNN to 1270 mm year^{-1} or above in the mountainous regions (Jones and Fahl, 1994), and about 50% occurs as snowfall (Brabets et al., 2000). The glacierized area, which was specified by Landsat images on 1 and 3 August 2005 (resolution, 30 m), occupies ca. 5.6% of the basin area upstream of point TNN, and the other (non-glacierized) regions consist mostly of forests (51%) and wetlands (9%) with discontinuous permafrost, with the remaining area being mostly shrublands and barren.

The vegetation in the Tanana River basin is dominated by the needle leaf forest (e.g., black spruce and white spruce) and broad leaf forest (e.g., aspen). Above the tree line, herbaceous and barren areas are dominant. The observation site (point PC) in Phelan Creek is located 2 km downstream of the toe of Gulkana Glacier. The drainage area upstream of point PC is 31.6 km^2, of which ca. 63% is covered by Gulkana Glacier (March 2000), and the others by debris with no vegetation. The altitude upstream of point PC ranges from 1100 to 2430 m a.s.l. The mean slopes upstream of points TNN, CHE, and PC are 11.1°, 11.8°, and 16.5°, respectively. In the Tanana River basin, the river is frozen from late October to late April. When air temperature is above freezing from late April onward, the snowmelt event starts, and as a result, the river ice breaks up. According to the duration and magnitude of positive air temperature and snow accumulation, the snowmelt discharge varies in the snowmelt period of late April to May or early June. Glacier melt, which occurs from June to September, fluctuates daily and seasonally depending on the variation in air temperature and the location of the snowline on the glacier surface, which changes the area of different albedo on glacier.

Observations

In this study, the hydrological conditions of 2008 are investigated in detail by dividing the year into the frozen, snowmelt, and glacier-melt periods. At points TNN, CHE, and PC, temporal variations of suspended sediment concentration (SSC) were obtained from June 2007 to September 2008 by frequent river water sampling. The river water sampling was performed at points

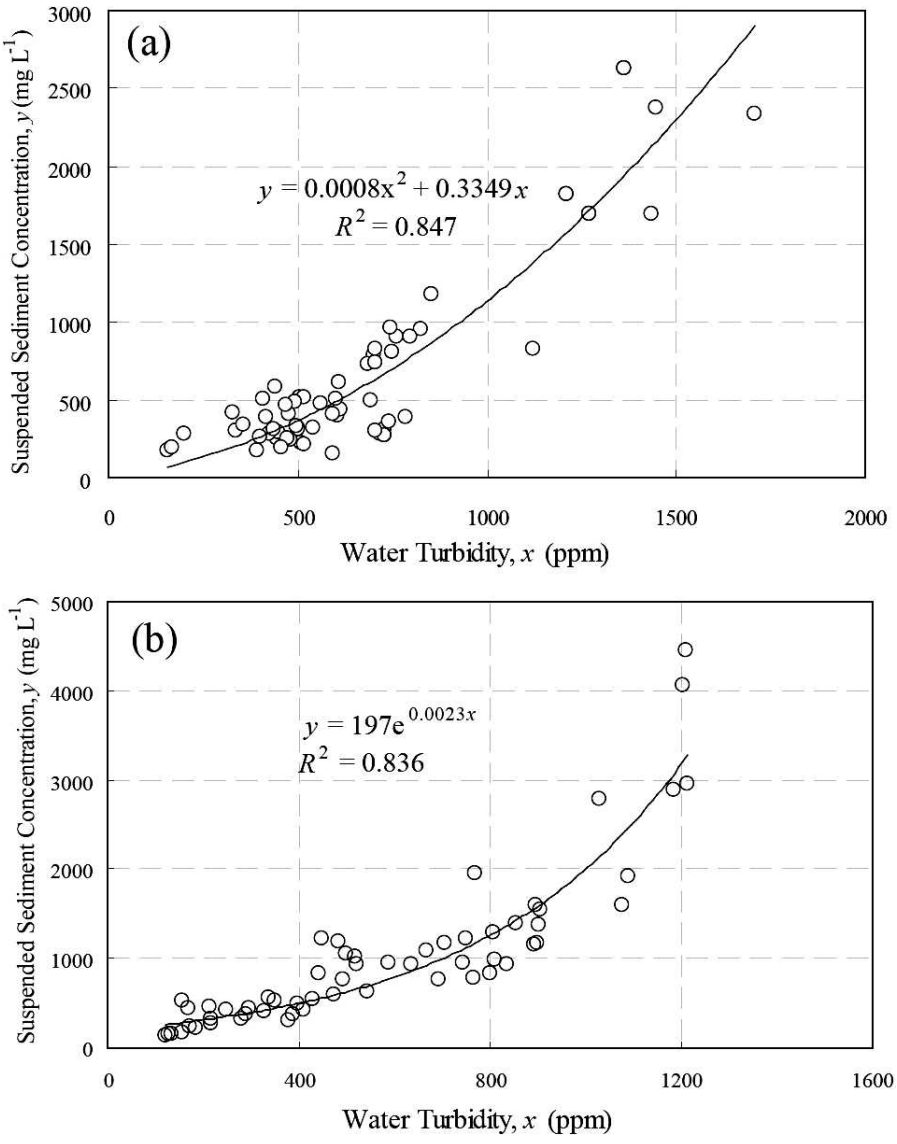

FIGURE 2. Relationship between water turbidity (ppm) and suspended sediment concentration (SSC, mg L^{-1}) at (a) point PC and (b) point TNN.

TNN and CHE once a week during non-rainfall periods, and once everyday to every three days during snowmelt and rainfall events. At point PC, river water was sampled five times and three times in the glacier-melt seasons of 2007 and 2008, respectively. The river water samples were filtered by GF/C filters (pore size: 1.2 μm). The SSC of sampled water was obtained by drying the filters at 90 °C for three hours or more, and weighing them. The dried samples were burned at 600 °C for 3 hours or more to remove organic matter, and then the dry samples were weighted again. The ratios between the reduced mass and SSC were calculated as ignition loss. At points TNN and PC, river water turbidity was monitored by using self-recording turbidimeters at 1 hr intervals for June–September of 2000–2007, and in April–September 2008. The recorded turbidity time series were converted to SSC time series by the high correlation ($R^2 = 0.847$ and $P < 0.01$ for 64 samples at point PC; $R^2 = 0.836$ and $P < 0.01$ for 58 samples at point TNN) between turbidity and simultaneous SSC of river water (Fig. 2).

River discharge data at the three points were obtained from the U.S. Geological Survey Water Data for the Nation (http://water-data.usgs.gov/nwis/). There are 15 weather stations of the National Oceanic and Atmospheric Administration, Western Regional Climate Center (WRCC) and the Alaska Climate Research Center in or around the Tanana River basin (Fig. 3 and Table 1). The data

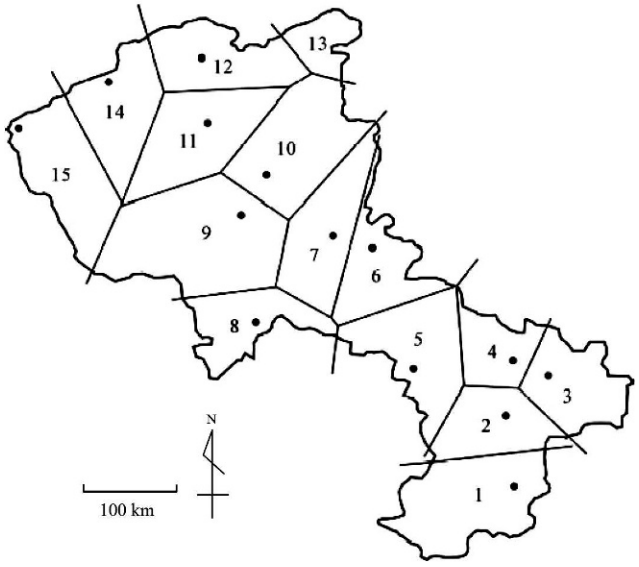

FIGURE 3. Location of 15 weather stations in or around the Tanana River basin, which is partitioned by the Thiessen method (Chikita et al., 2007).

TABLE 1

List of weather station numbers and names, the elevation at each weather station, averaged elevation of each Thiessen area, monthly precipitation at each weather station in June and averaged monthly precipitation in each Thiessen area in June.

No. and Name of weather stations	Latitude	Longitude	Elevation (m a.s.l.) at each weather station	Averaged elevation (m a.s.l.) of each non-glacierized Thiessen area *1	Averaged elevation (m a.s.l.) of each glacierized Thiessen area *1	Monthly precipitation (mm) at each weather station in June *2	Averaged monthly precipitation (mm) in each non-glacierized Thiessen area in June *2	Averaged monthly precipitation (mm) in each glacierized Thiessen area in June *2
1 Chisana	62°08′00″N	142°05′00″W	1011	1606	2323	83	113	145
2 Jatahmund	62°36′00″N	142°05′00″W	701	952	1914	66	76	108
3 Alcan Hwy MI-1244	62°49′00″N	141°28′00″W	549	685		51	56	
4 Northway	62°58′09″N	141°54′18″W	525	601		46	53	
5 Tok	62°57′26″N	143°20′48″W	701	1045	2034	83	91	144
6 T Lake	63°45′12″N	143°49′00″W	632	739	2125	44	61	114
7 George Creek	63°50′15″N	144°21′01″W	465	863	2192	70	80	116
8 Paxson	62°56′43″N	145°30′05″W	823	1369	1985	83	113	136
9 Delta Junction	63°59′00″N	145°39′00″W	398	847	2225	66	99	142
10 Goodpasture	64°14′17″N	145°16′01″W	463	722		78	80	
11 Salcha	64°35′24″N	146°08′24″W	305	484		64	66	
12 Angel Creek	65°01′12″N	146°13′41″W	335	644		55	64	
13 Birch Creek	65°35′05″N	144°21′49″W	259	1032		39	77	
14 Fairbanks	64°50′12″N	147°36′54″W	138	221		48	48	
15 Nenana	64°34′13″N	148°49′44″W	122	555		47	62	

*1 Calculated from National Elevation Dataset.

*2 Obtained from monthly precipitation map of June averaged between 1961 and 1991 by the Climate Source, Inc.

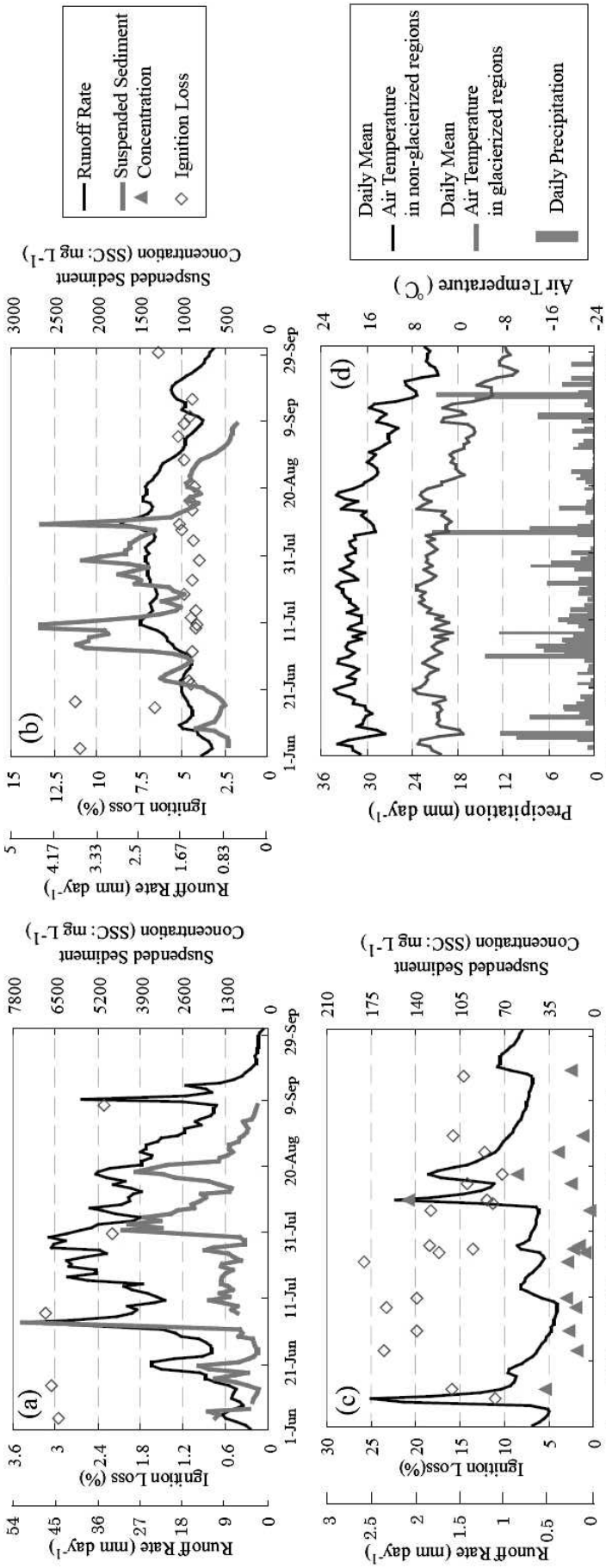

FIGURE 4. Temporal variations of runoff rate, suspended sediment concentration (SSC) and ignition loss at (a) point PC, (b) point TNN, and (c) point CHE; (d) daily precipitation, *P*; and daily mean air temperatures, T_g and T_{ng}, in June to September of 2007.

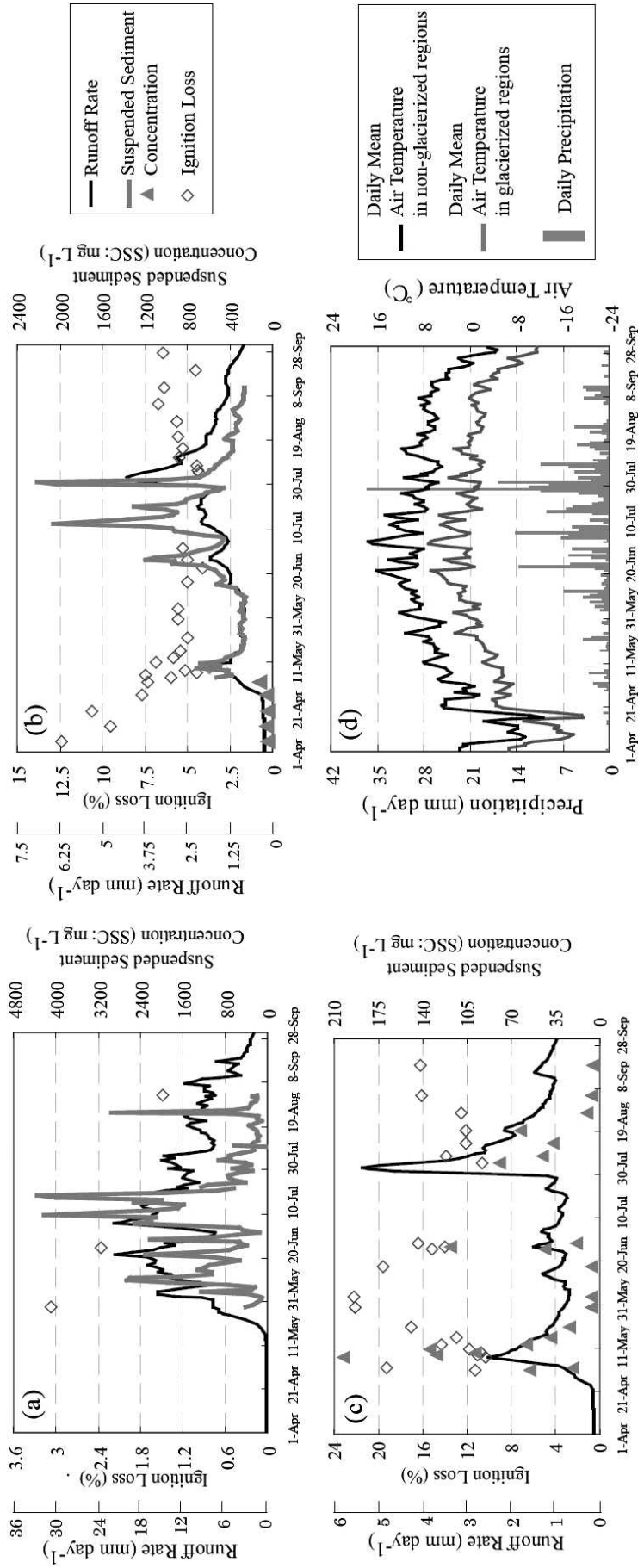

FIGURE 5. Temporal variations of runoff rate, suspended sediment concentration (SSC), and ignition loss at (a) point PC, (b) point TNN, and (c) point CHE; (d) daily precipitation, P; and daily mean air temperatures, T_g and T_{ng}, in April to September of 2008.

TABLE 2

Daily runoff rate, mean suspended sediment concentration, daily suspended sediment yield, and mean ignition loss in the glacier-melt periods of 2007 and 2008, in the frozen and snowmelt period of 2008, and in the hydrological year of October 2007 to September 2008.

Glacier-melt period (June to September 2007)	TNN	CHE	PC
Daily Runoff Height (mm day^{-1})	1.9	0.9	21.4
Mean Suspended Sediment Concentration (mg L^{-1})	1107	39	1716
Daily Suspended Sediment Yield (t km^{-2} day^{-1})	2.1	0.034	37.0
Mean Ignition Loss (%)	5.2	16.5	2.7
Ice-covered Period (October 2007 to April 2008)	TNN	CHE	PC
Daily Runoff Height (mm day^{-1})	0.3	0.1	0.2
Mean Suspended Sediment Concentration (mg L^{-1})	45	3.0	-
Daily Suspended Sediment Yield (t km^{-2} day^{-1})	0.013	0.0004	-
Mean Ignition Loss (%)	10.7	33.2	-
Snowmelt Period (May 2008)	TNN	CHE	PC
Daily Runoff Height (mm day^{-1})	1.1	1.1	0.2
Mean Suspended Sediment Concentration (mg L^{-1})	370	65	-
Daily Suspended Sediment Yield (t km^{-2} day^{-1})	0.407	0.072	-
Mean Ignition Loss (%)	5.5	12.3	-
Glacier-melt Period (June to September 2008)	TNN	CHE	PC
Daily Runoff Height (mm day^{-1})	1.7	1.2	11.2
Mean Suspended Sediment Concentration (mg L^{-1})	625	39	1114
Daily Suspended Sediment Yield (t km^{-2} day^{-1})	1.1	0.044	12.5
Mean Ignition Loss (%)	5.3	15.1	2.3
Hydrological Year (October 2007 to September 2008)	TNN	CHE	PC
Daily Runoff Height (mm day^{-1})	0.9	0.6	4.2
Mean Suspended Sediment Concentration (mg L^{-1})	456	35	996
Daily Suspended Sediment Yield (t km^{-2} day^{-1})	0.41	0.021	4.19
Mean Ignition Loss (%)	5.4	14.5	2.3

of daily precipitation and daily mean temperature at the weather stations were provided by these agencies. The area controlled by meteorological conditions at each weather station was determined by the Thiessen method (Chikita et al., 2006, 2007; Wada, 2010). The failure of data records at each weather station was complemented by the correlation with the data obtained near the station ($P < 0.05$). The Thiessen areas were separated into 2 arc sec mesh, in order to consider the elevation effect on air temperature and precipitation patterns. The differences of elevation between the weather station and each mesh were calculated from the National Elevation Dataset (NED), and air temperatures at each mesh were computed by applying the temperature lapse rate (0.65 °C per 100 m) to the differences of elevation (March, 2000). The precipitation of each gridcell was calculated as observed precipitation at the weather station multiplied by the ratio between the mean precipitation at each mesh and that at the weather station, which were obtained from the mean monthly precipitation map of June during 1961 to 1991 provided by Climate Source, Inc. (http://www.climatesource.com/map_gallery.html).

Observational Results

Figures 4 and 5 show the time series of daily runoff rate, daily mean suspended sediment concentration, ignition loss, daily precipitation, and daily mean air temperature in June to September 2007 and in April to September 2008, respectively. The daily runoff rate is here defined as the daily water discharge divided by the drainage area upstream of each gauging station. The use of the runoff rate allows us to directly compare hydrological conditions of river basins with different areas. The frozen period corresponds to a period before the discharge increase in late April, and the snowmelt period to a period of the runoff events in late April to May or early June without much precipitation. Glacier melt occurs from June to September, following the snowmelt period. The discharge at point PC increased in June and July, and then decreased in August and September, corresponding to the air temperature variation in the glacierized regions. The discharge at point CHE then consisted of stable base flow (about 0.5 mm day^{-1}) augmented with rainfall runoff. The mean daily runoff rate in the glacier-melt periods of 2007 and 2008 was 1.8 mm day^{-1} at point TNN, 1.1 mm day^{-1} at point CHE, and 16.3 mm day^{-1} at point PC (Table 2). The runoff rate at point PC is thus 15 times and 9 times as high as that at point CHE and point TNN, respectively. The baseflow at point TNN increased in June and July, and decreased in August and September, coinciding with the seasonal variations of discharge at point PC. This suggests that the glacier-melt discharge is a significant source of the water discharge at point TNN.

The SSC values averaged over the glacier-melt periods of 2007 and 2008 were 1415 mg L^{-1} at point PC, 866 mg L^{-1} at point TNN, and 39 mg L^{-1} at point CHE, while the mean ignition loss was then 2.5% at point PC, 5.3% at point TNN, and 15.8% at point CHE (Table 2). The ignition loss at point PC was thus about one sixth as high as that at point CHE, but the SSC at point PC was 36 times as large as that at point CHE. This suggests that the concentration of particulate organic matter at point PC is above that at point CHE in spite of no vegetation in the glacierized regions. Also, the low ignition loss at point TNN, compared with that at point CHE, suggests that the glacial sediment with the relatively low ignition loss is a main constituent of suspended sediment at point TNN.

Using the significant correlations ($R^2 = 0.45$ to 0.92, $P < 0.05$) between the discharge and the sediment load at observation points, the mean daily suspended sediment yield (t km^{-2} day^{-1}) in the glacier-melt periods of 2007 and 2008 was calculated at 24.8 t km^{-2} day^{-1} at point PC, 0.039 t km^{-2} day^{-1} at point CHE, and 1.6 t km^{-2} day^{-1} at point TNN. The sediment yield at point TNN (mean slope, 11.1°; basin area, 6.63×10^4 km^2 upstream of point TNN) is thus 41 times as high as that at point CHE (mean slope, 11.8°; basin area, 5.40×10^3 km^2). Generally, steep and

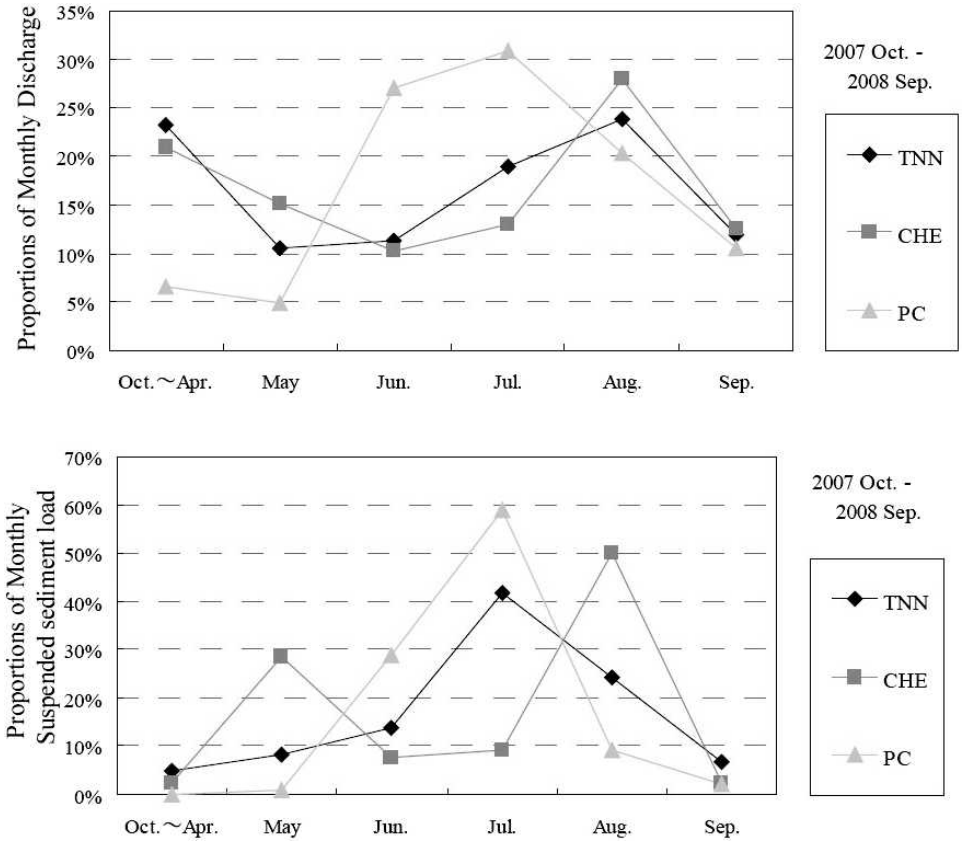

FIGURE 6. Proportion (%) of monthly discharges (upper) and monthly sediment loads (lower) at points PC, CHE, and TNN in October 2007 to September 2008.

small basins have high sediment yield (De Boer and Crosby, 1996; Koppes and Montgomery, 2009), but the TNN basin is more gentle and larger than the CHE basin. Meanwhile, the sediment yield at point PC is 640 times as high as that at point CHE. The high sediment yield at point TNN is thus explained by the high sediment yield from the glaciation in glacierized regions. Hence, the glacierized region, accounting for 5.6% of the basin area upstream of point TNN, is judged to be a major source of the sediment yield at point TNN.

With increasing temperature, the snowmelt runoffs without much precipitation occurred at points TNN and CHE from late April to May 2008. The snowmelt runoff at point PC started in late May because of the high altitude (1100 to 2430 m a.s.l.). The SSC at point TNN varied between 270 mg L^{-1} and 720 mg L^{-1}, while the SSC at point CHE ranged from ca. 50 mg L^{-1} to ca. 200 mg L^{-1} during the snowmelt period. The mean daily suspended sediment yield at point TNN was 0.407 t km^{-2} day^{-1}, being much higher than 0.072 t km^{-2} day^{-1} at point CHE. The mean ignition loss was then 5.5% at point TNN and 12.3% at point CHE. The relatively high sediment yield and low ignition loss at point TNN during non–glacier melt suggests that fluvial erosion of glacial sediment along the channels of the Tanana River and its glacier-fed tributaries dominate the sediment transport.

The runoff rate in the frozen period before late April was lowest at all the observation points over the hydrological year (on average, about 0.3 mm day^{-1} at point TNN, about 0.1 mm day^{-1} at point CHE, and about 0.2 mm day^{-1} at point PC). At point PC, the discharge was then barely traceable because of low air temperatures. At point TNN, the SSC was also lowest at 39–54 mg L^{-1}. Mean daily sediment yield was 12.6 kg km^{-2} day^{-1} at point TNN and 0.4 kg km^{-2} day^{-1} at point CHE. The relatively high sediment yield and low ignition loss at point TNN is similar to those in the snowmelt period. Thus, it is suggested that, during the frozen period, the glacial sediment in the channels is fluvially eroded.

Figure 6 shows the proportion of monthly discharge and monthly sediment load at points PC, CHE, and TNN in October 2007 to September 2008. At point PC, 78% of the annual discharge and most of the suspended sediment load occurred in the glacier-melt period of June to September. At point CHE, 15% of the annual discharge and 29% of the suspended sediment load occurred in the snowmelt period of May. At point TNN, the proportion of monthly discharge is on the whole similar to that at point CHE, but the monthly sediment load in the snowmelt period occupies only 8% of the annual sediment load. The proportion of monthly sediment load at point TNN was at its maximum of 42% in July, when the monthly discharge and sediment load at point PC peaked. In late July to early August, the largest flood for the last 40 years occurred on the Tanana River (Plumb and Rundquist, 2009). The discharge at point CHE then increased greatly (Fig. 3). As a result, 50% of the annual sediment load at point CHE occurred in August. At point TNN, the monthly sediment load then accounted for 24%, which was lower than in July. Hence, it is found that, at point TNN, the impact of sediment load by the large flood is low compared with that by consistent glacier melt.

The annual mean daily sediment yield in October 2007 to September 2008 was 4.19 t km^{-2} day^{-1} at point PC and 0.021 t km^{-2} day^{-1} at point CHE. The annual mean daily sediment load at point PC was thus about 200 times as large as that at point CHE. Meanwhile, the annual mean daily sediment yield at point TNN was 0.41 t km^{-2} day^{-1}. Hence, as the glaciers

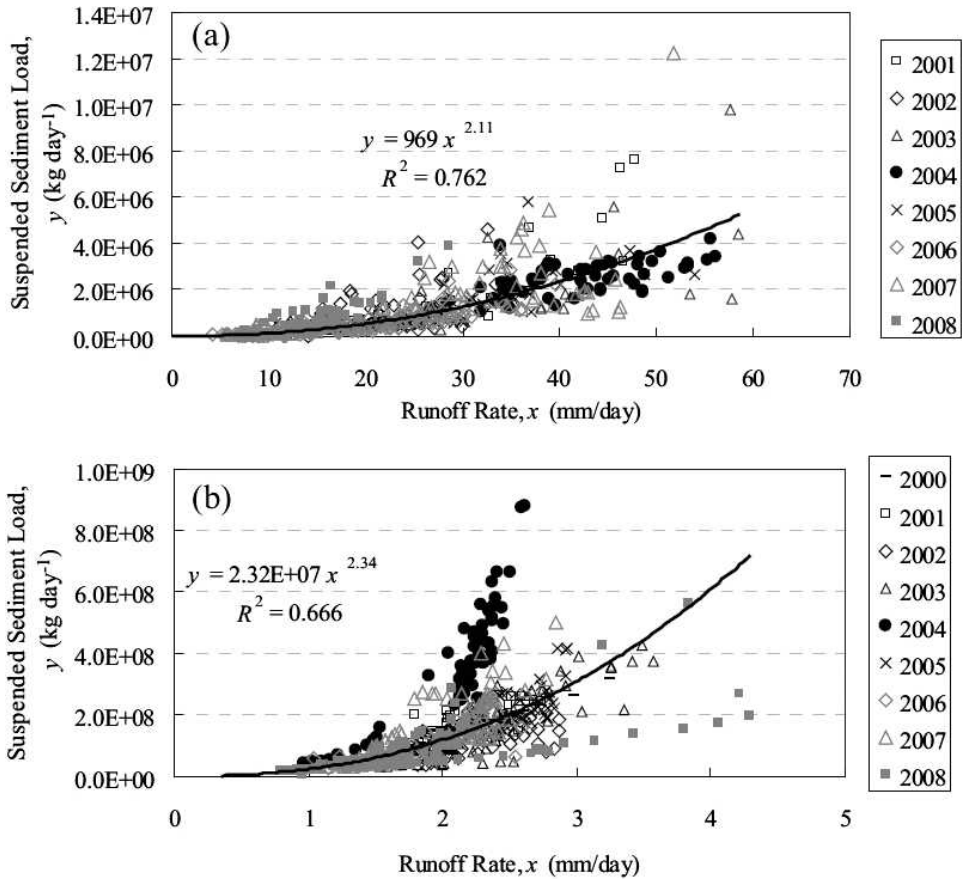

FIGURE 7. Relations between runoff rate and suspended sediment yield at (a) point PC and (b) point TNN in the glacier-melt periods of 2001 to 2008 and 2000 to 2008, respectively.

shrink by global warming (e.g., Matsuo and Heki, 2010) and decrease in glacial dynamic activity, the sediment yield at point TNN may approach that at point CHE.

Figure 7 shows relations between the daily runoff rate and sediment yield at (a) point PC and (b) point TNN in the glacier-melt periods of 2000 to 2008 or 2001 to 2008. The correlations are significant ($R^2 = 0.762$ and $P < 0.01$ at point PC and $R^2 = 0.666$ and $P < 0.01$ at point TNN). The relatively low correlation at point TNN (Fig. 7, b) resulted from the very high sediment load in 2004 and the low sediment load in 2008, compared with the other years. The high and low sediment loads appear to have occurred because of extremely high and relatively low air temperatures in the glacierized regions, respectively (Fig. 8). The sediment load at point TNN thus likely depends on both the discharge at point TNN and the glacier-melt discharge from the glacierized regions. Hence, to investigate how the discharge from the glacierized regions seasonally contributes to the TNN sediment load, it is important to know the processes of fluvial sediment transport.

Figure 8 shows relations between the mean air temperature over the glacierized regions and the total sediment load or the total runoff rate over the glacier-melt periods of 2000 to 2008 or 2001 to 2008. At point PC, the linear relationship between the mean air temperature and the total runoff rate or total sediment load (Fig. 8, a) is evident with the significant correlation ($R^2 = 0.827$, $P < 0.01$, or $R^2 = 0.686$, $P = 0.01$). This indicates that the air temperature in the glacierized regions is the main driver for changes in both the discharge and suspended sediment load at point PC. Especially, the extremely warm temperatures in 2004 produced the highest runoff rate and suspended sediment load at point PC. The slope of the regression lines in Figure 8, part a, offers daily values of 6.4 mm day^{-1} °C^{-1} for the runoff rate and 13.7 t km^{-2} day^{-1} °C^{-1} as the sediment yield for the sediment load.

The total runoff rate at point TNN (Fig. 8, b) was nearly constant for the air temperature variation in the glacierized regions ($R^2 = 0.047$, $P = 0.56$). Meanwhile, the correlation between mean daily air temperature in the glacierized regions and the total sediment load at point TNN was significant at $R^2 = 0.526$ and $P = 0.03$. The total runoff rates at point TNN over the glacier-melt period were similar at 228 mm in 2004 and at 208 mm in 2008, but the total sediment load of 2004 was ca. 4 times higher than that of 2008. This means that the contribution of sediment load from the glacierized regions is much higher than that from non-glacierized regions.

The high air temperature in the glacierized regions produces both high glacier-melt discharge and high evapotranspiration in the river basin. In addition, the high air temperature in the glacierized regions usually occurs under conditions of fine weather or low precipitation. Hence, quantitative estimate of the water balance for the Tanana River basin and a runoff analysis are needed to quantify the contribution of glacier-melt discharge to the discharge and sediment load at point TNN.

Water Balance Calculations

The water balance of the Tanana River basin upstream of point TNN was estimated for the glacier-melt periods of 2000 to 2008.

BASIC EQUATIONS

The water balance in the glacier-melt period is obtained by the following equation:

$$\Delta S_{sum} = P_{sum} + Mg_{sum} + F_{sum} - Q_{sum} - ET_{sum}, \quad (1)$$

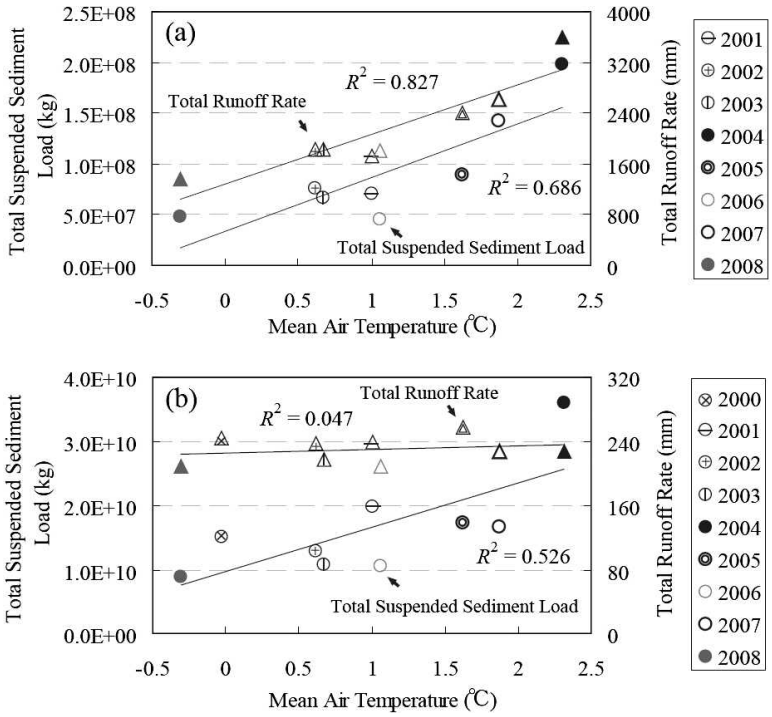

FIGURE 8. Relations between air temperature, total sediment load, and total runoff rate at (a) point PC and (b) point TNN in the glacier-melt periods of 2001 to 2008 and 2000 to 2008 (circles for the sediment load and triangles for the runoff rate).

where ΔS_{sum} is the temporal change of groundwater and glacier storage (mm), P_{sum} is the total precipitation (mm), Mg_{sum} is the total glacier-melt amount (mm), F_{sum} is the total permafrost-melt amount (mm), Q_{sum} is the total runoff rate (mm) at point TNN, and ET_{sum} is the total actual evapotranspiration (mm). Here, the elevation-corrected daily precipitation, P, (Figs. 4 and 5) was applied to the P_{sum} calculation. The ET_{sum} values were obtained by the following Pikes' equation (Dingman, 2002):

$$ET_{sum} = \frac{P_{sum}}{\sqrt{1 + (P_{sum}/PET_{sum})^2}}, \quad (2)$$

where PET_{sum} is the sum of the daily potential evapotranspiration, PET (mm day^{-1}), by the Hamon method (Hamon, 1963). As a result, the calculated evapotranspiration ratio, $\gamma = ET_{sum}/PET_{sum}$, was 0.63 ± 0.14 (mean ± STD). The total glacier-melt amount, Mg_{sum}, was calculated by the following degree-day approach (Braithwaite, 1995):

$$Mg = f \cdot T_a, \quad (3)$$

where Mg is the daily glacier-melt amount (mm day^{-1}), f is the degree-day factor (mm day^{-1} °C^{-1}), and T_a is the daily mean air temperature. The degree-day factor, f, depends on physical conditions of the glacier, especially the glacial surface, which varies seasonally from snow to ice with different albedo; f = 3.5 to 5.0 and f = 7.0 to 10.0 (mm day^{-1} °C^{-1}) were obtained for the snow-covered and ice-covered areas of the Gulkana Glacier upstream of point PC, respectively (March, 2000). According to the results of Kido et al. (2007) for the Gulkana Glacier, f = 3.5 and f = 7.0 (mm day^{-1} °C^{-1}) were here adopted for the snow- and the ice-covered areas, respectively. The snowline, a boundary between the upper snow-covered area and the lower ice-covered area on the glacier surface, was supposed to be located at the altitudes of 1350 m a.s.l. before 15 June, 1500 m a.s.l. for 1–31 July, and 1700 m a.s.l. after 1 August in the glacierized regions upstream of point TNN (Kido et al., 2007). Narita (2007) calculated the melt amount of the Gulkana Glacier over the glacier-melt seasons of 2004 and 2005 by the degree-day method and the heat balance method. As a result, the difference of the total glacier-melt amount between the two methods was 7.3%. Hence, the adoption of the degree-day method seems to be reasonable.

The glacierized region was determined from two Landsat images dated early August 2005. As a result, the snow-covered areas outside the glacierized region before early August were ignored. Thus, the glacier-melt amount was probably underestimated in June and July and overestimated in August and September. The daily mean air temperature, T_a, was calculated by applying the temperature lapse rate to the National Elevation Dataset (NED) of the glacierized regions. The resolution of calculation was 2 arc sec. The total glacier-melt amount, Mg_{sum}, in Equation (1) was obtained by summing the obtained daily glacier-melt rate, Mg, for the glacier-melt period. Finally, the temporal change of groundwater storage, ΔS_{sum}, and the total permafrost-melt amount, F_{sum}, in Equation (1) were estimated as the residual in the water balance.

ESTIMATED RESULTS

Table 3 shows the calculated mean daily water balance in the glacier-melt periods of 2000 to 2008. As a result, the daily values of precipitation, glacier-melt amount, evapotranspiration, and runoff rate averaged over 2000–2008 were 2.24 ± 0.44, 0.70 ± 0.17, 1.33 ± 0.13, and 1.91 ± 0.14 mm day^{-1} ± STD, respectively, and thus the glacier-melt amount was 31% of the precipitation. The mean daily evapotranspiration of 1.33 ± 0.13 mm day^{-1} was similar to that in the Yukon river basin in June to August (1.73 ± 0.53 mm day^{-1} for broadleaf forest, 1.19 ± 0.27 mm day^{-1} for needleleaf forest, and 1.40 ± 0.24 mm day^{-1} for grassland) established by Yuan et al. (2010). The residual of the input minus the output was –0.31 ± 0.25 mm day^{-1} ± STD, which is equal to the volumetric change of water storage, ΔS, plus the permafrost-melt amount, F. The negative small value of the residual (9.5% of total output) means that the permafrost-meltwater and/or the stored water are drained, and that the influence of ΔS and F on the water balance is relatively low.

TABLE 3

Mean daily precipitation, *P*, glacier-melt amount, *Mg*, actual evapotranspiration, *ET*, runoff rate, *Q*, and the residual in the glacier-melt periods of 2000 to 2008.

(mm day^{-1})	2000	2001	2002	2003	2004	2005	2006	2007	2008	Mean	STD	STD (%)
Precipitation *P*	2.63	1.78	2.63	2.00	1.39	2.22	2.37	2.49	2.67	2.24	0.44	19.7
Glacier-melt *Mg*	0.58	0.67	0.60	0.71	1.05	0.76	0.65	0.83	0.45	0.70	0.17	24.4
Total Input	3.21	2.45	3.23	2.71	2.44	2.98	3.02	3.32	3.12	2.94	0.33	11.3
Evapotranspiration *ET*	1.46	1.18	1.41	1.23	1.12	1.35	1.39	1.50	1.38	1.33	0.13	9.7
Runoff rate *Q*	2.04	1.99	1.98	1.81	1.90	2.15	1.74	1.89	1.73	1.91	0.14	7.3
Total Output	3.50	3.18	3.39	3.04	3.02	3.49	3.13	3.39	3.11	3.25	0.19	5.9
P+Mg-ET	1.76	1.26	1.82	1.48	1.32	1.63	1.63	1.82	1.74	1.61	0.21	13.0
Residual	−0.29	−0.73	−0.15	−0.33	−0.58	−0.51	−0.11	−0.07	0.00	−0.31	0.25	82.0

Simulations of Discharge and Sediment Load

MODELING

In order to quantify the contribution of glacier melt to the discharge at point TNN, the discharge time series in the glacier-melt periods of 2000 to 2008 were simulated by a water tank model (Sugawara, 1972). This model is a conceptual, lumped model for river runoff analysis, but has so far simulated reasonably glacier melt, snowmelt, and rainfall runoffs (Kite, 2001; Hagg et al, 2006; Kido et al., 2007; Chikita et. al., 2007). The HVB-ETH model of Braun and Renner (1992) for river runoffs including glacier-melt discharge and the linear reservoir model of Hannah and Gurnell (2001) for glacier-melt runoffs are the same in principle as the tank model. Many distributed models such as TOPMODEL have succeeded in rainfall runoff simulations, but not so in daily snowmelt runoffs (Dery et al., 2005; Hollander et al., 2009). In the tank model, it is supposed that a river basin consists of several combined tanks. In this study, the Tanana River basin was separated into three subbasins, in order to consider the elapsed time of river flow and the dampening of flood waves in the downstream (Fig. 9). The "Subbasin 2" (or "Subbasin 3") in Figure 9 was divided into "Section 2" (or "Section 4") with a unique tank, and "Section 3" (or "Section 5") with three serial tanks. The tank in each of Section 2 and Section 4, called "a

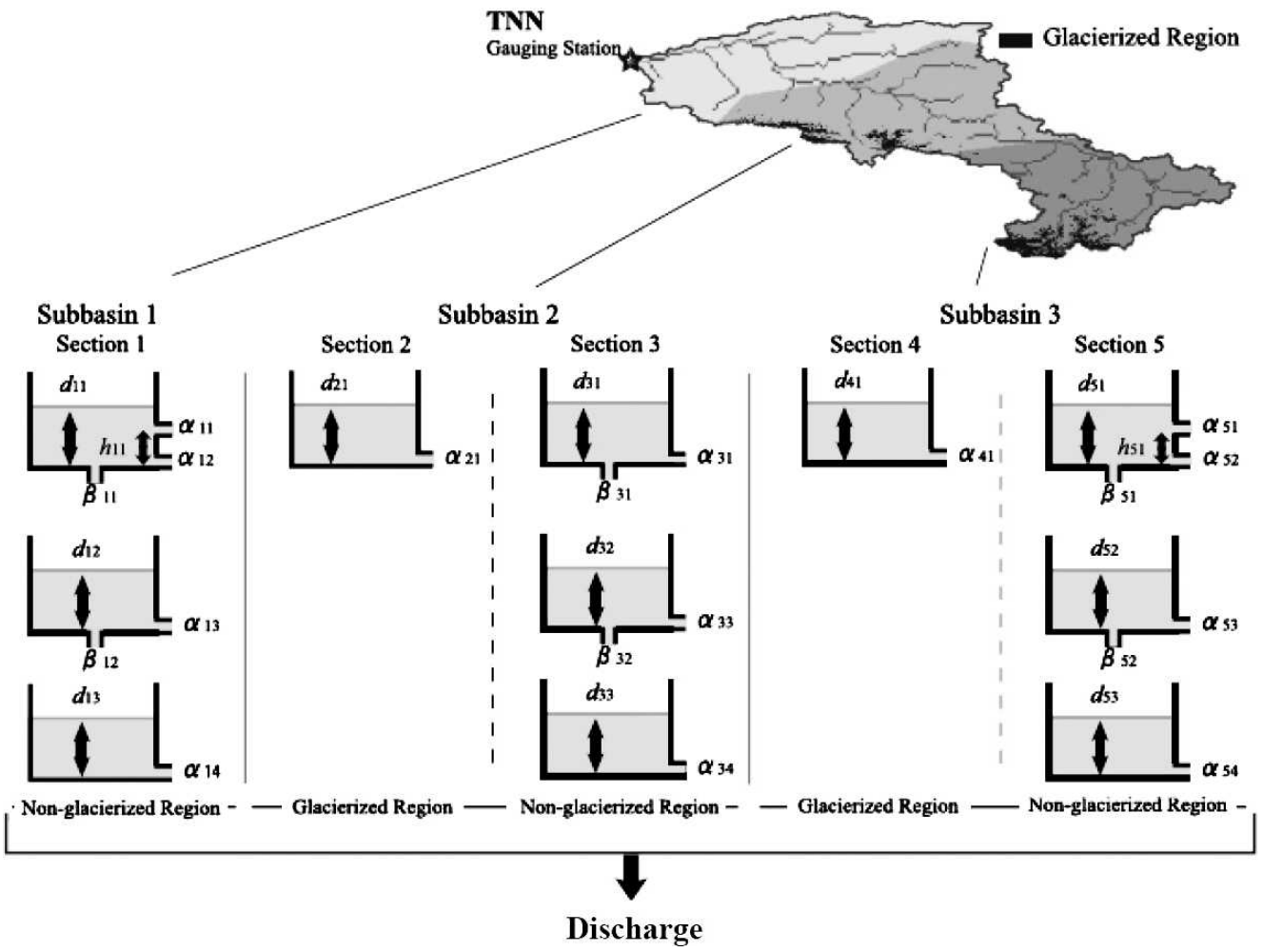

FIGURE 9. Tank layout for the Tanana River basin (see text for more detail).

glacial tank," corresponds to glacierized regions in each of Subbasin 2 and Subbasin 3, respectively, while the three tanks in each of Section 1, Section 3, and Section 5, called "non-glacial tanks," correspond to the non-glacierized regions with permafrost in each of "Subbasin 1," "Subbasin 2," and "Subbasin 5," respectively. The tank layout for glacierized and non-glacierized regions was decided by considering the characteristics of glacial and non-glacial discharges in the subarctic drainage basin, respectively (Woo and Marsh, 2005; Chikita et. al., 2006; Kido et. al., 2007). The discharges from the top, middle, and bottom tanks in the non-glacierized regions correspond to the surface flow, intermediate flow, and base flow, respectively. The non-glacial top tank and the glacial tank are recharged by rainfall in the non-glacierized regions and by glacier melt and rainfall in the glacierized regions, respectively. The daily rainfalls and glacier-melt amount obtained in the water balance of Equation (1) were then applied as the water input to the tanks. The daily actual evapotranspiration, *ET*, was given as the output from the non-glacial, top, and middle tanks. The evapotranspiration from the glacierized regions was assumed to be negligible, because of the relatively low air temperature. The drains of stored water and permafrost-melt discharge, which were calculated as residual in the water balance (ca. 9.5% of the total output in Table 3), were relatively low, and thus were contained in the initial water depth of the bottom tank. After the calculation of the recharge and output of water, the discharge from each tank was computed with a time step of 1 hour by the following equations:

$$q_{ij} = a_{ij}\left(d_{ij}(t) - h_{ij}\right)\left(d_{ij}(t) > h_{ij}\right) \tag{4}$$

and

$$q_{ij} = 0\left(d_{ij}(t) < h_{ij}\right), \tag{5}$$

where q_{ij} is the simulated discharge (mm h^{-1}), α_{ij} is the discharge ratio, $d_{ij}(t)$ is the water depth (mm) of a tank at a time, t, h_{ij} is the height (mm) of the discharge hole, and i and j are the numbers of the tank or hole (i = 1 to 5, j = 1 to 4). The infiltrations from each of the top and middle tanks were simultaneously calculated by:

$$I_{ij} = \beta_{ij} \cdot d_{ij}(t), \tag{6}$$

where I_{ij} (mm h^{-1}) is the infiltration to the lower tank, and β_{ij} is the infiltration rate (h^{-1}). The delayed times of Subbasins 1, 2, and 3 were set at 1 day, 2 days, and 3 days, respectively. According to the observed results of Kido et al. (2007), a response of glacier melt to the air temperature was lagged by 2 days. The calculation was carried out for periods of May to September in 2000 to 2008, but May was set as a preliminary calculation period. The parameters, α_{ij}, β_{ij}, and h_{ij}, and the initial water depth, $d_{ij}(0)$, were determined to give the best fit to the observed discharge time series of 2002. The obtained parameter sets were applied to the other years' time series, since the parameters reflect the sedimentary structure and initial water storage of the Tanana River basin, thus being peculiar to the drainage basin.

As shown by Figure 7, the relations between runoff rate and suspended sediment load are approximately obtained by the following power function, called the *L-Q* equation (Walling, 1974; Morgan, 1995; Asselman, 2000; Kido et al., 2007):

$$L = aQ^b, \tag{7}$$

where L is the suspended sediment load (kg day^{-1}), Q is the runoff rate (mm day^{-1}), and a and b are empirical coefficients. The source of suspended sediment at point TNN is assumed to be located in glacierized regions, non-glacierized regions, and river channels. The sediment source in the channels is based on the fluvial erosion of glacial sediment deposited previously in the channels. Hence, the suspended sediment load, L_{TNN} (kg day^{-1}), at point TNN is the sum of the suspended sediment load from the glacierized regions, L_g, the non-glacierized regions, L_{ng}, and fluvial resuspension of sediment along the channels of the Tanana River and its glacial tributaries, L_b. Each of L_g, L_{ng}, and L_b can be shown by such a power function as Equation (7):

$$L_{TNN} = a_1 {Q_g}^{b1} + a_2 {Q_{ng}}^{b2} + a_3 {Q_{TNN}}^{b3}, \tag{8}$$

where Q_g, Q_{ng}, and Q_{TNN} are the runoff rates (mm day^{-1}) from the glacierized regions and non-glacierized regions and at point TNN, respectively, a_i and b_i (i = 1, 2, 3) are empirical coefficients. The non-glacierized regions account for 94.4% of the Tanana River basin, but the sediment yield (0.044 t km^{-2}) in the glacier-melt period of 2008 at point CHE is of nearly the order of 10^3 lower than that (12.5 t km^{-2}) at point PC. Hence, the sediment load, L_{ng} or $a_2 {Q_{ng}}^{b2}$, from the non-glacierized regions can be here neglected. The simulation of the discharge time series allows us to separate the TNN discharge into the discharge from the glacierized regions and that from the non-glacierized regions. Thus, at first, the discharge, Q_g in Equation (8) was obtained by the runoff analysis. The coefficients b_1 and b_3 were set at a constant of 2.2, according to observational results (Fig. 7). The coefficients a_1 and a_3 were determined to give the best fit to the observed sediment load series in each year.

SIMULATION RESULTS

Figure 10 shows comparisons between the calculated and observed discharges in the glacier-melt periods of (a) 2004, (b) 2007, and (c) 2008. The calculated discharges from the glacierized regions and the non-glacierized regions are also shown. As a result, in the calculation periods of 2000 to 2008, the root mean square error (RMSE) between the simulated and observed results ranged from 9% to 23% of the observed, mean daily discharge with the Nash-Sutcliffe efficiency coefficients (NSE) of 0.35 to 0.84 (Nash and Sutcliffe, 1970), in spite of the parameter values common to all the years (Wada, 2010). The RMSE of 42 peak discharges of 2000 to 2008 was 15% of the mean observed peak discharges. The RMSE between total simulated and observed runoff in the glacier-melt periods was 10% of the mean total observed runoff. Thus, the estimate of the water balance and the simulation of the discharge time series at point TNN were reasonable. This means that discharge time series at point TNN can be simulated well from meteorological data only.

The discharge from the glacierized regions contains glacier-melt discharge and rainfall runoff. The glacier-melt discharge, Q_{gm}, is calculated by following equation:

$$Q_{gm} = Q_g \times M_g / \left(M_g + P_g\right), \tag{9}$$

where Q_{gm} is the glacier-melt discharge and P_g is the precipitation in the glacierized regions. As a result, the contribution of glacier-melt discharge to the total discharge at point TNN ranged from 26% to 57% with an average of 40% (Table 4). The glacierized regions are thus an important source of water input to the Tanana River basin, in spite of the limited 5.6% glacial cover. The highest air temperature and lowest rainfall in 2004 caused the highest contribution (57%) of the glacier-melt discharge, while the year 2008 was coldest and wettest, thus generating the lowest contribution of 26%. The contribution of glacier-melt discharge to river discharge has so far been estimated at 8–66% for five river basins of 7–55% glacial cover in the northern Tien Shan (Hagg

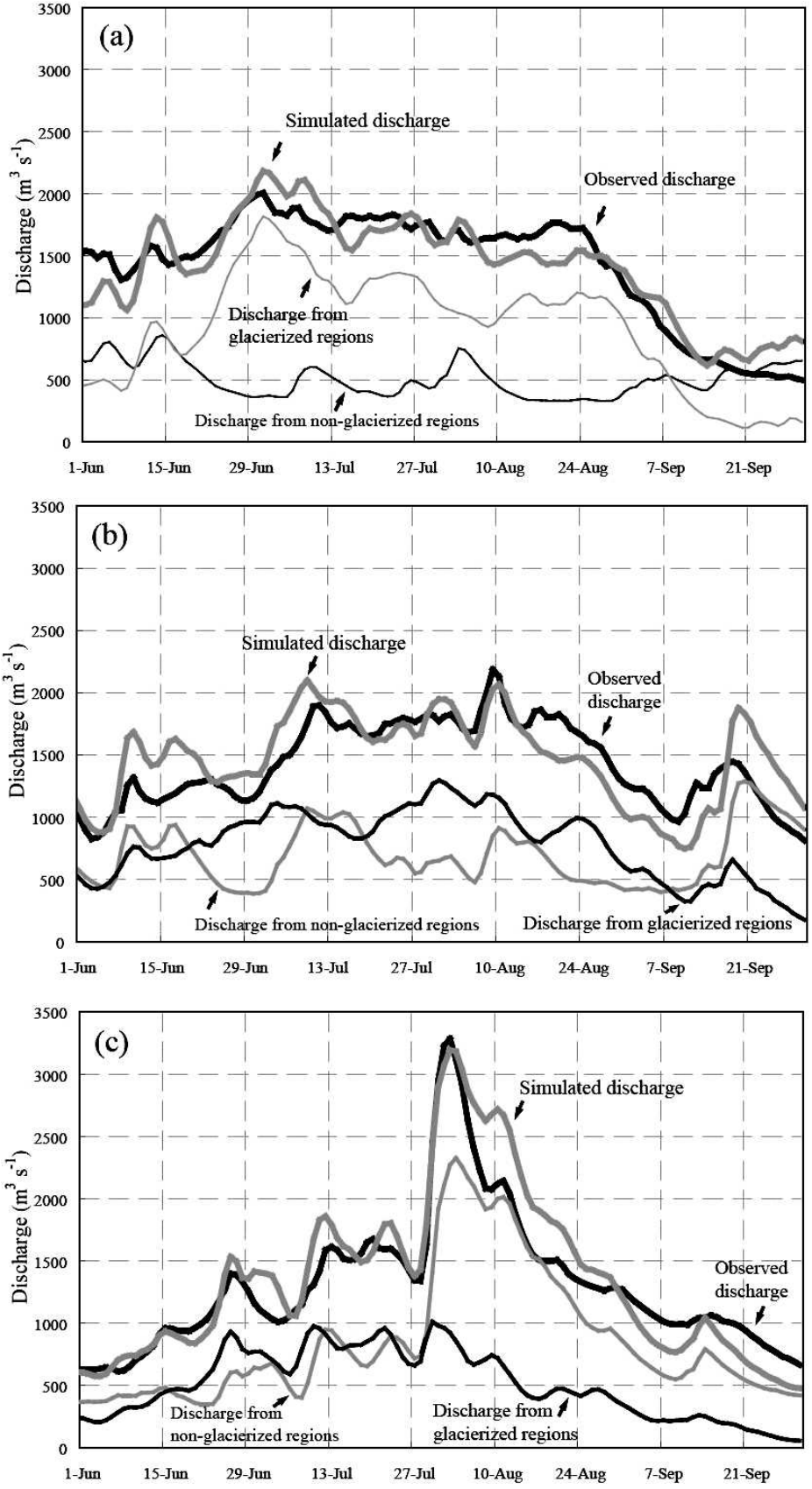

FIGURE 10. Comparison between observed and simulated results for the discharge time series at point TNN in the glacier-melt periods of (a) 2004, (b) 2007, and (c) 2008 (see text for more detail).

TABLE 4

Contributions of glacier-melt discharge to the total discharge at point TNN. Mean air temperature over the glacierized regions, mean observed runoff rate at point TNN, the root mean square errors (RMSE), and the Nash-Sutcliffe efficiency coefficients (NSE) are also shown.

	2000	2001	2002	2003	2004	2005	2006	2007	2008
Contribution of glacier-melt discharge (%)	31	42	34	40	57	43	40	44	26
Mean air temperature (°C) in the glacierized regions	0.0	1.0	0.6	0.7	2.3	1.6	1.1	1.9	−0.3
Mean runoff rate (mm day^{-1}) at point TNN	2.01	1.96	1.94	1.78	1.87	2.11	1.71	1.86	1.71
RMSE (mm day^{-1})	0.47	0.43	0.18	0.27	0.23	0.39	0.39	0.32	0.29
RMSE (%)	23	22	9	15	12	19	23	17	17
NSE	−0.47	0.52	0.81	0.84	0.84	0.35	0.45	0.45	0.84

et al., 2006), and at 70–88% for two stream basins of 8.7% and 18.9% glacial cover in Oregon, U.S.A. (Nolin et al., 2010).

Figure 11 shows secular relations between the basin-scaled precipitation, total simulated glacier-melt runoff, total simulated rainfall runoff, total simulated runoff at point TNN, observed runoff at point TNN, and air temperature averaged over each glacier-melt period of 2000 to 2008. The glacier-melt runoff and rainfall (or non-glacial) runoff are here expressed as the runoff rate (mm). The total runoff at point TNN in the glacier-melt period was 230 ± 16 mm ± STD averaged in 2000 to 2008. The total glacier-melt runoff increased linearly at the rate of 23 mm 1 °C^{-1}. Meanwhile, the precipitation and the rainfall runoff tend to decrease with increasing air temperature (−40 and −20 mm 1 °C^{-1}, respectively). The variation of the total rainfall runoff (Mean ± STD =134 ± 20 mm) was smaller than that of the precipitation (274 ± 53 mm). This suggests that the groundwater storage in the river basin buffers the rainfall runoffs. The increase of the glacier-melt runoff with increasing air temperature can cancel the decrease of the rainfall runoff. The total runoff of the Tanana River is thus relatively stable (230 ± 16 mm).

Figure 12 shows comparisons between the simulated and observed results for the sediment load time series at point TNN in (a) 2004, (b) 2007, and (c) 2008. The sediment load time series of 2000, 2001, and 2006 were not simulated because of the short recordings of water turbidity. All the Nash-Sutcliffe efficiency coefficients (NSE) were positive with a range of 0.41 to 0.82, though the RMSE values were relatively large at 29 to 63% of the mean daily sediment load (Table 5). The mean simulated sediment load of 25 peaks was 75% of the mean observed sediment load. The underestimated peaks occurred mainly under rainfall events. Hence, the fluvial resuspension of glacial deposits by rainfall runoff may be underestimated. The RMSE between the total observed and simulated sediment load was 11% of the mean total sediment load. For the simulations in Table 5, the coefficients, a_3, b_1, and b_3, were fixed as constants of 3.45×10^6, 2.2, and 2.2. The coefficient a_1 covers a relatively small range of 1.36×10^5 to 1.51×10^5 except 2.32×10^5 in 2004. These suggest that the sediment erodibility, indicated by b_1 and b_3, is constant, and that the sediment availability for erosion, shown by a_1 and a_3, is stable (Walling, 1974; Morgan, 1995; Asselman, 2000; Kido et al., 2007). The highest glacier-melt discharge in 2004 was produced by the highest air temperature in the calculation years (Table 4). The extremely high glacier-melt discharge can produce the high stage of proglacial streams and the active migration of the stream channels. As a result, the large a_1 value in 2004 is probably due to the fluvial erosion of proglacial sediment accumulated in the previous years.

The highest contribution (94%) and the lowest contribution (76%) of sediment load from the glacierized regions appear in the hottest year 2004 and in the coolest and wettest year 2008, respectively. This provides evidence that a major source of fluvial sediment in the Tanana River basin is located in the glacierized regions, and that the total discharge from the glacierized regions mainly determines the total sediment load at point TNN in the glacier-melt period, in spite of the 5.6% glacial cover. The simulation also revealed that the total sediment load at point TNN increases by 6.9×10^6 t 1 °C^{-1}. The mean daily sediment yield by fluvial resuspension at point TNN was 251 kg day^{-1} km^{-2}, which is about 6 times as large as at non-glacial point CHE (44 kg day^{-1} km^{-2}). This means that the fluvial resuspension of erodible glacial deposits in or around the glacier-fed river channels occurs actively much more than fluvial erosion in the non-glacierized regions.

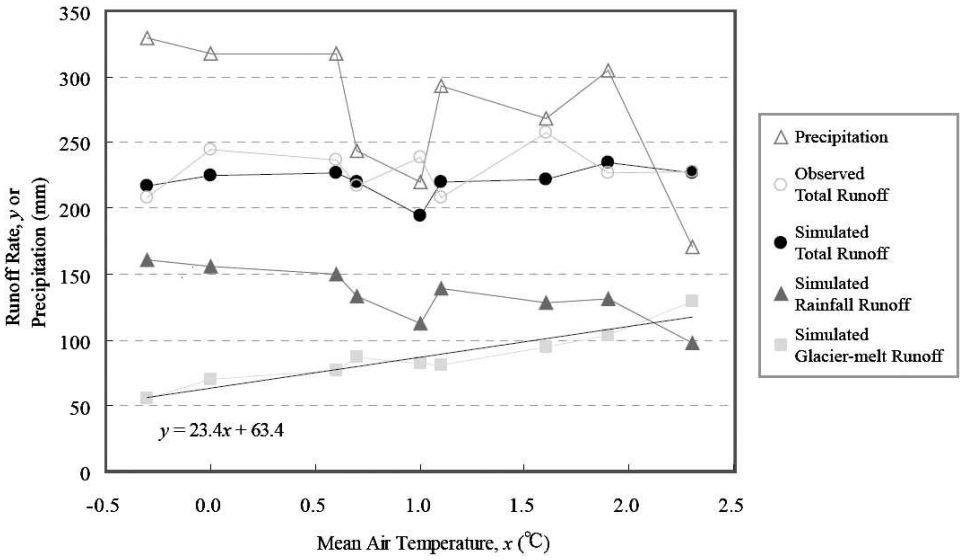

FIGURE 11. Secular relations between the basin-scaled precipitation, total simulated glacier-melt runoff, total simulated rainfall runoff, total simulated runoff at point TNN and observed runoff at point TNN, and air temperature averaged over the glacier-melt periods of 2000 to 2008.

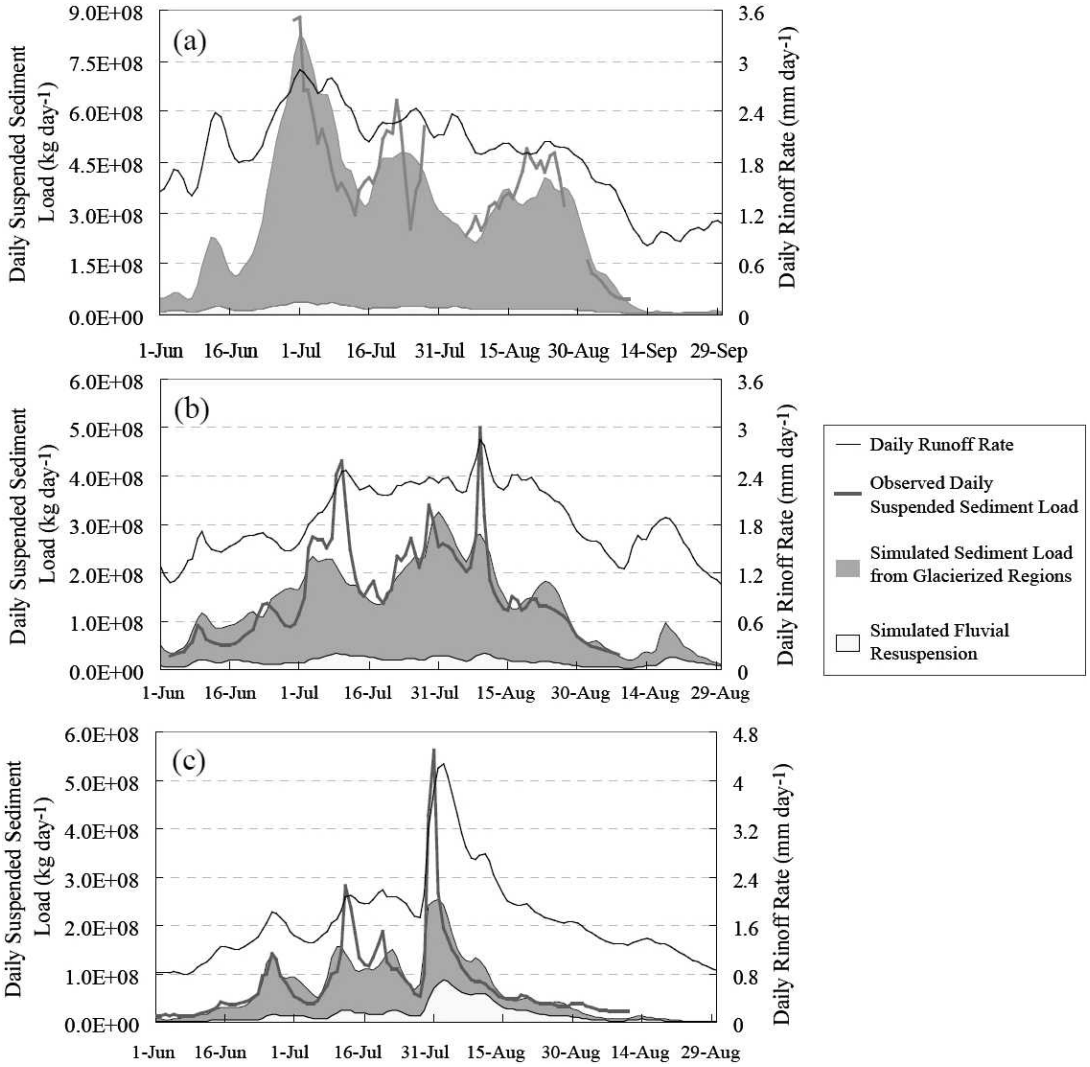

FIGURE 12. Simulated results for suspended sediment load series at point TNN and from the glacierized regions, and fluvial resuspension in or around river channels in the glacier-melt periods of (a) 2004, (b) 2007 and (c) 2008. The daily runoff rate at point TNN is also shown.

Conclusions and Future Work

In this study, the characteristics of temporal variations of river discharge and suspended sediment load over a hydrological year (frozen period of October to late April, snowmelt period of late April to May or early June, and glacier-melt period of June to September) were investigated by field observations, and the contributions of discharge and sediment load from glacierized regions and non-glacierized regions to those of the Tanana River were quantified by a water tank model and the empirical discharge-sediment load rating curves, *L-Q* equations. In the glacier-melt period, the contributions of glacier-melt discharge and sediment load from the glacierized regions, which comprise only 5.6% of the Tanana River basin, to discharge and sediment load of the Tanana River varied between 26% and 57% and between 76% and 94%, respectively, mainly depending on the air temperature in

TABLE 5

Contributions of suspended sediment load from the glacierized regions and fluvial resuspension in or around the river channels in the Tanana River basin. The coefficient a_1, observed mean daily suspended sediment load at point TNN, and the root mean square errors (RMSE) and the Nash-Sutcliffe efficiency coefficients (NSE) are also shown.

	2002	2003	2004	2005	2006	2007	2008
Contribution of Glacierized Regions (%)	83	85	94	87	—	87	76
Contribution of Resuspension (%)	17	15	6	13	—	13	24
Coefficient a_1 (10^5)	1.36	1.50	2.32	1.45	—	1.51	1.51
Mean Daily Suspended Sediment Load (10^6 kg day^{-1})	105	88	295	141	86	137	71
RMSE (10^6 kg day^{-1})	39	49	87	65	—	53	45
RMSE (%)	37	56	29	46	—	39	63
NSE	0.50	0.82	0.77	0.41	—	0.70	0.70

the glacierized regions. Other contribution to the sediment load is probably due to the fluvial resuspension of glacial deposits in or around the river channels.

These results imply that, over the coming decade, as global warming continues, the discharge and sediment load of the Tanana River may increase by 23 mm 1 $^{\circ}C^{-1}$ and 6.9×10^6 t 1 $^{\circ}C^{-1}$, respectively. Meanwhile, on the time scale of several decades, the glaciers' shrinkage due to global warming (Matsuo and Heki, 2010) may ultimately decrease the sediment supply to the river. If the glaciers completely disappear in the Tanana River basin, subglacial sediment will be missing but easily erodible glacial tills and debris will remain. Hence, the sediment yield in the Tanana River basin (150 t km^{-2} $year^{-1}$ from Table 2) is probably still higher than in the Siberian river basins (1.8 to 8.3 t km^{-2} $year^{-1}$), but may equilibrate that in the Yukon (72.2 t km^{-2} $year^{-1}$) and Mackenzie (66.5 t km^{-2} $year^{-1}$) river basins, which have the glacierized-area ratio much smaller than does the Tanana River basin. In this study, the secular change of the glacierized area was not taken into account. The long-term monitoring of discharge and water turbidity and the modeling of large time scale are needed to clarify the effect of the glacial shrinkage on the sediment load.

Acknowledgments

We are greatly indebted to Prof. S.-D. Kim for his useful information on the vegetation in Alaska. We express our gratitude to Prof. M. Sasaki, Dr. H. Iwana, Dr. E. Watanabe, and Mr. W.-J. Kim for their great help in our field observations. We also appreciate the support of Prof. S. Akasofu, Prof. L. Hinzman, Prof. M. Fukuda, and Ms. Yoriko Freed; the International Arctic Research Center (IARC); the University of Alaska at Fairbanks (UAF); and we appreciate the data supplied by the U.S. Geological Survey, Western Regional Climate Center and Alaska Climate Research Center. This study was financially supported by the Japan Aerospace Exploration Agency (JAXA) as research in the joint project of IARC/JAXA.

References Cited

Asselman, H., 2000: Fitting and interpretation of sediment rating curves. *Journal of Hydrology*, 234: 228–248.

Brabets, T. P., Wang, B., and Meade, R. H., 2000: Environmental and hydrologic overview of the Yukon river basin, Alaska and Canada. *U.S. Geological Survey Water-Resources Investigations Report*, 99-4204: 106 pp.

Braithwaite, R. J., 1995: Aerodynamic stability and turbulent heat flux over a melting ice surface, the Greenland ice sheet. *Journal of Glaciology*, 41: 562–571.

Braun, L. N., and Renner, C. B., 1992: Applications of a conceptual runoff model in different physiographic regions of Switzerland. *Hydrological Sciences Journal*, 73: 217–231.

Carson, M. A., Jasper, J. N., and Conly, F. M., 1998: Magnitude and sources of sediment input to the Mackenzie Delta, Northwest Territories, 1974–1994. *Arctic*, 51: 116–124.

Chikita, K. A., Richard, K., and Kumai, R., 2002: Characteristics of sediment discharge in the subarctic Yukon river, Alaska. *Catena*, 48: 235–253.

Chikita, K. A., Morita, T., Wada, T., and Kido, D., 2006: Discharge and sediment load from a subarctic river basin: Tanana River, Alaska. *Journal of the Japanese Association of Hydrological Science*, 36: 59–69.

Chikita, K. A., Wada, T., Kudo, I., Kido, D., Narita, T., and Kim, Y., 2007: Modeling discharge, water chemistry and sediment load from a subarctic river basin: the Tanana River, Alaska. *IAHS Publications*, 314: 45–56.

Chikita, K. A., Kaminaga, R., Kudo, I., Wada, T., and Kim, Y., 2010: Parameters determining water temperature of a proglacial stream: the Phelan Creek and the Gulkana Glacier, Alaska. *River Research and Applications*, 26: 995–1004.

De Boer, D. H., and Crosby, G., 1996: Specific sediment yield and drainage basin scale. *In* Walling, D. E., and Webb, B. W. (eds.), *Erosion and Sediment Yeild: Global and Regional Perspectives (Proceedings of the Exeter Symposium, July 1996)*. Wallingford, U.K.: IAHS Press, *IAHS Publication*, 236: 333–338.

Dery, S. J., Salomonson, V. V., Stieglitz, M., Hall, D. K., and Appel, I., 2005: An approach to using snow areal depletion curves inferred from MODIS and its application to land surface modelling in Alaska. *Hydrological Processes*, 19: 2755–2774.

Dingman, S. L., 2002: *Physical Hydrology*. 2nd edition. Englewood Cliffs, New Jersey, U.S.A.: Prentice-Hall.

Ferrians, O. J., 1965: Permafrost map of Alaska: *U.S. Geological Survey Miscellaneous Geologic Investigations Map*, I-445: scale 1:2,500,000.

Global Carbon Project, 2006: Carbon Cycle Policy Brief, Report No. 5. Grigny, France: Imprimerie Technique Conseil.

Guo, L., and Macdonald, R. W., 2006: Source and transport of terrigenous organic matter in the upper Yukon river: evidence from isotope ($\delta^{13}C$, $\Delta^{14}C$, and $\delta^{15}N$) composition of dissolved, colloidal, and particulate phases. *Global Biogeochemical Cycles*, 20: GB2011, doi:10.1029/2005GB002593.

Hagg, W., Braun, L. N., Weber, M., and Becht, M., 2006: Runoff modelling in glacierized Central Asian catchments for present-day and future climate. *Nordic Hydrology*, 37: 93–105.

Hamon, R. W., 1963: Computation of direct runoff amounts from storm rainfall. Wallingford, U.K.: IAHS Press, *IAHS Publication*, 63.

Hannah, D. M., and Gurnell, A. M., 2001: A conceptual, linear reservoir runoff model to investigate melt season changes in cirque glacier hydrology. *Journal of Hydrology*, 246: 123–141.

Hasholt, B., and Mernild, S. H., 2008: Hydrology, sediment transport and water resources of Ammassalik Island, SE Greenland. *Geografisk Tidsskrift–Danish Journal of Geography*, 108(1): 73–95.

Hasholt, B., Bobrovitskaya, N., Bogen, J., McNamara, J., Mernild, S. H., Milburn, D., and Walling, D. E., 2006: Sediment transport to the Arctic Ocean and adjoining cold oceans. *Nordic Hydrology*, 37(4–5): 413–432.

Hay, L. E., and McCabe, G. J., 2010: Hydrologic effects of climate change in the Yukon river basin. *Climatic Change*, 100: 509–523.

Hollander, H. M., Blume, T., Bormann, H., Buytaert, W., Chirico, G. B., Exbrayat, J.-F., Gustafsson, D., Holzel, H., Kraft, P., Stamm, C., Stoll, S., Bloschl, G., and Fluhler, H., 2009: Comparative predictions of discharge from an artificial catchment (Chicken Creek) using sparse data. *Hydrology and Earth System Sci*ences, 13: 2069–2094.

Jones, S. H., and Fahl, C. B., 1994: Magnitude and frequency of floods in Alaska and conterminous basins of Canada. *U.S. Geological Survey Water-Resources Investigations Report*, 93-4179: 122 pp.

Kido, D., Chikita, K. A., and Hirayama, K., 2007: Subglacial drainage system changes of the Gulkana Glacier, Alaska: discharge and sediment load observations and modeling. *Hydrological Processes*, 21: 399–410.

Kite, G., 2001: Modelling the Mekong: hydrological simulation for environmental impact studies. *Journal of Hydrology*, 253: 1–13.

Knudsen, N. T., Yde, J. C., and Gasser, G., 2007: Suspended sediment transport in glacial meltwater during the initial quiescent phase after a major surge event at Kuannersuit Glacier, Greenland. *Danish Journal of Geography*, 107(1): 1–7.

Koppes, M. N., and Montgomery, D. R., 2009: The relative efficacy of fluvial and glacial erosion over modern to orogenic timescales. *Nature Geoscience*, 2: 644–647.

Lammers, R. B., Shiklomanov, A. I., Vörösmatry, C. J., Fekete, B. M., and Peterson, B. J., 2001: Assessment of contemporary

arctic river runoff based on observational discharge records. *Journal of Geophysical Research*, 106: 3321–3334.

March, R. S., 2000: Mass balance, meteorological, ice motion, surface altitude, runoff and ice thickness data at Gulkana Glacier, Alaska, 1995 balance year. *U.S. Geological Survey Water-Resources Investigations Report*, 00-4074.

Matsuo, K., and Heki, K., 2010: Time-variable ice loss in Asian high mountains from satellite gravimetry. *Earth and Planetary Science Letters*, 290: 30–36.

McClelland, J. W., Déry, S. J., Peterson, B. J., Holmes, R. M., and Wood, E. F., 2006: A pan-arctic evaluation of changes in river discharge during the latter half of the 20th century. *Geophysical Research Letters*, 33: L06715, doi:10.1029/2006GL025753.

Meybeck, M., and Ragu, A., 1996: River discharges to the oceans: an assessment of suspended soils, major ions and nutrients. Environment information and assessment report. Nairobi, Kenya: U.N. Environment Programme, 250 pp.

Morgan, R. P. C., 1995: *Soil Erosion and Conservation.* 2nd edition. London: Longman.

Narita, Y., 2007: The interannual hydrological variability in an Alaskan glacier-covered drainage basin. M.Sc. thesis, Hokkaido University, Japan, 34 pp.

Nash, J. E., and Sutcliffe, J. V., 1970: River flow forecasting through conceptual models part I–A discussion of principles. *Journal of Hydrology*, 10: 282–290.

Nolin, A. W., Phillippe, J., Jefferson, A., and Lewis, S. L., 2010: Present-day and future contributions of glacier runoff to summertime flows in a Pacific Northwest watershed: implications for water resources. *Water Resources Research*, 46: doi:10.1029/2009WR008968.

Overeem, I., and Syvitski, J. P. M., 2008: Changing sediment supply in arctic rivers. *Sediment Dynamics in Changing Environments (Proceedings of a Symposium Held in Christchurch, New Zealand, December 2008)*. Wallingford, U.K.: IAHS Press, *IAHS Publication*, 325: 391–397.

Overeem, I., and Syvitski, J. P. M., 2010: Shifting discharge peaks in arctic rivers, 1977–2007. *Geografiska Annaler*, 92: 285–296.

Plumb, E., and Rundquist, L., 2009: The 2008 Tanana River flood: where did all the water come from? *American Water Resources Association 2009 Spring Specialty Conference, Managing Water Resources Development in a Changing Climate*, May 4–6, 2009, Anchorage, Alaska.

Stafford, J. M., Wendler, G., and Curtis, J., 2000: Temperature and precipitation of Alaska: 50 year trend analysis. *Theoretical and Applied Climatology*, 67: 33–44.

Striegel, R. G., Dornblaser, M. M., Aiken, G. R., Wickland, P., and Raymond, P. A., 2007: Carbon export and cycling by the Yukon, Tanana, and Porcupine rivers, Alaska, 2001–2005. *Water Resources Research*, 43: doi: 10.1029/2006WR005201.

Sugawara, M., 1972: *A Method for Runoff Analysis*. Tokyo: Kyoritsu Shuppan Press (in Japanese).

Wada, T., 2010: Sediment load and chemical flux in the subarctic Tanana river basin, Alaska. PhD thesis, Hokkaido University, Japan, 93 pp.

Walling, D. E., 1974: Suspended sediment and solute yields from a small catchment prior to urbanization. *In* Gregory, K. J., and Walling, D. E. (eds.), *Fluvial Processes in Instrumented Watersheds*. London, U.K.: Institute of British Geographers, *Special Publication*, 6: 169–192.

Walling, D. E., and Webb, B. W., 1996: Erosion and sediment yield: a global overview. *In* Walling, D. E., and Webb, B. W. (eds.), *Erosion and Sediment Yield: Global and Regional Perspectives (Proceedings of the Exeter Symposium, July 1996)*. Wallingford, U.K.: IAHS Press, *IAHS Publication*, 236: 3–19.

Woo, M.-K., and Marsh, P., 2005: Snow, frozen soils and permafrost hydrology in Canada, 1999–2002. *Hydrological Processes*, 19: 215–229.

Yuan, W., Liu, S., Liu, H., Randerson, J. T., Yu, G., and Tieszen, L. L., 2010: Impacts of precipitation seasonality and ecosystem types on evapotranspiration in the Yukon river basin, Alaska. *Water Resources Research*, 46: doi:10.1029/2009WR008119.

MS accepted May 2011